

Single-electron capture and transfer ionization in collisions of Li^{3+} ions with helium

Ivan Mančev

Department of Physics, University of Niš, P. O. Box 224, 18001 Niš, Yugoslavia

(Received 14 June 2000; published 6 June 2001)

The total cross sections for single-electron capture and transfer ionization are computed for $\text{Li}^{3+} + \text{He}$ collisions in a four-body distorted-wave formalism. The contribution from the $e-e$ interaction during the collision is evaluated. Comparison between the present theoretical results and measurements at 50–5000 keV/amu yields satisfactory agreement. The continuum distorted-wave four-body method employed can provide information about the relative significance of the dynamic interelectron interaction in the collisions under study.

DOI: 10.1103/PhysRevA.64.012708

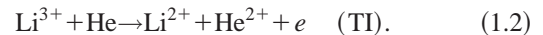
PACS number(s): 34.70.+e, 82.30.Fi

I. INTRODUCTION

In the past decade much attention has been paid to electron-electron correlation effects in ion-atom collisions. The simplest case where we can study these effects is a collision in which a bare nucleus P of charge Z_P is impinging upon a heliumlike atomic system consisting of two electrons e_1 and e_2 initially bound to the target nucleus T of charge Z_T , i.e., $Z_P + (Z_T; e_1, e_2)$ collisions. In such collisions, one-electron (electron capture, excitation, ionization) as well as two-electron transitions (double capture, double ionization, double excitation, simultaneous transfer and ionization, simultaneous transfer and excitation) can occur. Some two-electron processes are not negligible compared to single-electron transitions, in particular for multiply charged projectile ions. For example, the ratio of transfer ionization to single capture $R = \sigma_{\text{TI}}/\sigma_{\text{SC}}$ for F^{9+} incident on He [1] is 2.65, 1.75, and 1.0 at impact energy 0.5, 1.0, and 1.5 MeV/amu, respectively. The majority of the theoretical articles that have considered $Z_P + (Z_T; e_1, e_2)$ collisions employed the independent-particle model (IPM). In this model, there are many ways to approximate the wave function of a heliumlike atom. The approach in which an active electron of the two-electron target moves in an effective potential generated by a target nucleus and passive electron has frequently been used. Thus, in the IPM, the four-body problem is reduced to a three-body problem. Probabilities for one-electron transitions were combined to calculate cross sections for various one- and two-electron processes [2,3]. The main failure of the IPM is that dynamic (scattered) correlation effects are completely discarded from the outset. Hence, if we want to evaluate the role of the electron-electron interaction correlation we must deal with a four-body problem. Such four-body theories have been developed within the continuum distorted-wave (CDW-4B) formalism for double-electron capture [4–6], simultaneous transfer and ionization [7,8], and simultaneous transfer and excitation [9–11]. In addition to these two-electron transitions, the CDW-4B approximation was used in Refs. [12,13] for description of single-electron capture. The four-body first Born approximation with the correct boundary conditions (CB1-4B) was carried out for double-charge exchange [14,15], as well as for single-electron capture in collisions between two hydrogenlike atoms, where we can also evaluate the correlation effects [16,17]. There are second-order four-body hybrid theories

that are intermediate between the CDW-4B and CB1-4B approaches for double-charge exchange, termed the boundary-corrected continuum intermediate state [18] and Born distorted-wave methods [19]. The common property of all the quoted four-body theories is that these methods show systematic agreement with experimental data at intermediate and high impact energies.

In the present work, we shall apply the CDW-4B method to calculate total cross sections for single capture (SC) and transfer ionization (TI) for the following processes:



The reaction (1.1) has been theoretically treated previously by a number of authors using various methods. For example, the IPM and Roothan-Hartree-Fock (RHF) target screening were adopted within the corrected first Born theory of Belkić [20]. This gave good agreement with experimental data at intermediate and high impact energies. Belkić, Gayet, and Salin [21] originally introduced the RHF method for single-electron capture from a multielectron target within the CDW-3B approximation of Cheshire [22]. This RHF model and the CDW-3B approach were used by Saha, Data, and Mukherjee [23] for the charge-changing reaction (1.1) in the energy interval 0.2–4 MeV/amu. For the same collision system, theoretical total cross sections have also been obtained by Busnengo, Martinez, and Rivarola [24], using the continuum-distorted-wave-eikonal-initial-state (CDW-EIS) and the continuum-distorted-wave-eikonal-final-state (CDW-EFS) as well as the CDW-3B methods. These models treat the process (1.1) as a three-body problem and still the CDW-EIS model correctly predicted the behavior of the measured cross sections even at lower energies, while simultaneously achieving good agreement with high-energy experiments. Gravielle and Miraglia [25] studied reaction (1.1) using the prior form of the eikonal impulse approximation and assumed the IPM for the helium target. Sidorovich, Nikolaev, and McGuire [2] have applied the approximation of Bassel and Gerjuoy [26] to calculate the charge-changing cross sections in collisions of H^+ , He^{2+} , and Li^{3+} ions with He atoms in the energy region of 0.025–4 MeV/amu in the independent-electron approximation. The IPM and the unitarized distorted-wave approximation, which is based on the

atomic-orbital expansion, were used by Suzuki et al. [27] for description of the reaction (1.1). However, in their method the correlation term is simplified, according to $Z_T/r_1 - Z_T/r_2 + 1/r_{12} = -\alpha/r_1 - \alpha/r_2$ where α is the effective charge, so that their model cannot yield any information about the correlation effect. The reaction (1.2) was one of the subjects of investigation in Refs. [3], [2], [28] where an IPM was used.

Despite the availability of several theories, the contribution from the electron-electron interaction during the collision in $\text{Li}^{3+} + \text{He}$ scattering has not been previously assessed. Therefore, the main goal of the present work is an evaluation of the relative significance of the dynamic interelectron interaction in $\text{Li}^{3+} + \text{He}$ collisions by means of the CDW-4B theory. With regard to previous work [12,13], where a major influence of electronic correlations on electron capture to the ground state in $p + \text{He}$, $\text{He}^{2+} + \text{He}$, and $p + \text{Li}^+$ collisions was found, in the present paper the calculation is extended for charge exchange to the excited states, with the purpose of

determining whether electronic correlations remain important. In our discussion, emphasis will be placed upon the relative role of various terms in the full prior V_i and post V_f perturbations.

Atomic units will be used throughout unless otherwise stated.

II. THEORY

Let $\vec{s}_{1,2}$ and $\vec{x}_{1,2}$ be the position vectors of the electrons $e_{1,2}$ relative to Z_P and Z_T , respectively. Let e_1 be captured and e_2 be simultaneously ionized in the case of TI, whereas for SC e_2 stays bound to the target nucleus. We denote by \vec{R} the position vector of T with respect to P . The distance between electrons will be denoted by r_{12} . The transition amplitudes in the prior (−) and post (+) forms for transfer ionization and single capture in the CDW-4B theory can be written as [7,12]

$$T_{if}^{-(\text{TI})} = \mathcal{N} \int \int \int d\vec{R} d\vec{s}_1 d\vec{s}_2 e^{i\vec{\alpha}\cdot\vec{s}_1 + i\vec{\beta}\cdot\vec{x}_1 - i\vec{\kappa}\cdot\vec{x}_2} \varphi_{f_1}^*(\vec{s}_1) {}_1F_1(i\nu_T, 1, i\nu x_1 + i\vec{v}\cdot\vec{x}_1) {}_1F_1(i\zeta, 1, ipx_2 + i\vec{p}\cdot\vec{x}_2) \\ \times [V_P(R, s_2) {}_1F_1(i\nu_P, 1, i\nu s_1 + i\vec{v}\cdot\vec{s}_1) \varphi_i(\vec{x}_1, \vec{x}_2) - \vec{\nabla}_{x_1} \varphi_i(\vec{x}_1, \vec{x}_2) \cdot \vec{\nabla}_{s_1} {}_1F_1(i\nu_P, 1, i\nu s_1 + i\vec{v}\cdot\vec{s}_1) \\ - {}_1F_1(i\nu_P, 1, i\nu s_1 + i\vec{v}\cdot\vec{s}_1) (E_i - H_T) \varphi_i(\vec{x}_1, \vec{x}_2)], \quad (2.1)$$

$$T_{if}^{+(\text{TI})} = \mathcal{N} \int \int \int d\vec{R} d\vec{x}_1 d\vec{x}_2 e^{i\vec{\alpha}\cdot\vec{s}_1 + i\vec{\beta}\cdot\vec{x}_1 - i\vec{\kappa}\cdot\vec{x}_2} \varphi_i(\vec{x}_1, \vec{x}_2) {}_1F_1(i\nu_P, 1, i\nu s_1 + i\vec{v}\cdot\vec{s}_1) {}_1F_1(i\zeta, 1, ipx_2 + i\vec{p}\cdot\vec{x}_2) \\ \times \{ [V_P(R, s_2) + V(r_{12}, x_1)] {}_1F_1(i\nu_T, 1, i\nu x_1 + i\vec{v}\cdot\vec{x}_1) \varphi_f^*(\vec{s}_1) - \vec{\nabla}_{s_1} \varphi_f^*(\vec{s}_1) \cdot \vec{\nabla}_{x_1} {}_1F_1(i\nu_T, 1, i\nu x_1 + i\vec{v}\cdot\vec{x}_1) \}, \quad (2.2)$$

$$T_{if}^{-(\text{SC})} = N_{PT} \int \int \int d\vec{R} d\vec{x}_1 d\vec{x}_2 e^{i\vec{\alpha}\cdot\vec{s}_1 + i\vec{\beta}\cdot\vec{x}_1} \varphi_{f_1}^*(\vec{s}_1) \varphi_{f_2}^*(\vec{x}_2) {}_1F_1(i\nu_T, 1, i\nu x_1 + i\vec{v}\cdot\vec{x}_1) [V_P(R, s_2) \varphi_i(\vec{x}_1, \vec{x}_2) \\ \times {}_1F_1(i\nu_P, 1, i\nu s_1 + i\vec{v}\cdot\vec{s}_1) - \vec{\nabla}_{x_1} \varphi_i(\vec{x}_1, \vec{x}_2) \cdot \vec{\nabla}_{s_1} {}_1F_1(i\nu_P, 1, i\nu s_1 + i\vec{v}\cdot\vec{s}_1) - {}_1F_1(i\nu_P, 1, i\nu s_1 + i\vec{v}\cdot\vec{s}_1) \\ \times (E_i - H_T) \varphi_i(\vec{x}_1, \vec{x}_2)], \quad (2.3)$$

$$T_{if}^{+(\text{SC})} = N_{PT} \int \int \int d\vec{R} d\vec{x}_1 d\vec{x}_2 e^{i\vec{\alpha}\cdot\vec{s}_1 + i\vec{\beta}\cdot\vec{x}_1} \varphi_i(\vec{x}_1, \vec{x}_2) \varphi_{f_2}^*(\vec{x}_2) {}_1F_1(i\nu_P, 1, i\nu s_1 + i\vec{v}\cdot\vec{s}_1) \\ \times \{ [V_P(R, s_2) + V(r_{12}, x_1)] \varphi_{f_1}^*(\vec{s}_1) {}_1F_1(i\nu_T, 1, i\nu x_1 + i\vec{v}\cdot\vec{x}_1) - \vec{\nabla}_{s_1} \varphi_{f_1}^*(\vec{s}_1) \cdot \vec{\nabla}_{x_1} {}_1F_1(i\nu_T, 1, i\nu x_1 + i\vec{v}\cdot\vec{x}_1) \}, \quad (2.4)$$

where

$$V_P(R, s_2) = Z_P \left(\frac{1}{R} - \frac{1}{s_2} \right), \quad V(r_{12}, x_1) = \left(\frac{1}{r_{12}} - \frac{1}{x_1} \right). \quad (2.5)$$

The symbol ${}_1F_1(a, b, x)$ stands for the usual Kummer hypergeometric function. The momentum vector of the ejected electron e_2 with respect to its parent nucleus T is denoted by $\vec{\kappa}$. The wave function of the initial bound state is labeled by $\varphi_i(\vec{x}_1, \vec{x}_2)$, whereas $\varphi_{f_1}(\vec{s}_1)$ is the single-electron hydrogen-

like wave function of the Li^{2+} ion in the exit channel. The final bound state of He^+ in reaction (1.1) is described by $\varphi_{f_2}(\vec{x}_2)$. The remaining quantities in $T_{if}^{\pm(\text{TI})}$ and $T_{if}^{\pm(\text{SC})}$ are defined as follows:

$$\mathcal{N} = (2\pi)^{-3/2} N^{-*}(\zeta) N_{PT},$$

$$N_{PT} = N^+(\nu_P) N^{-*}(\nu_T),$$

$$N^-(\zeta) = \Gamma(1 + i\zeta) e^{\pi\zeta/2},$$

$$N^-(\nu_T) = \Gamma(1 + i\nu_T) e^{\pi\nu_T/2}, \quad N^+(\nu_P) = \Gamma(1 - i\nu_P) e^{\pi\nu_P/2},$$

$$\nu_P = \frac{Z_P}{v}, \quad \nu_T = \frac{Z_T - 1}{v}, \quad \zeta = \frac{Z_T}{p}, \quad \vec{p} = \vec{v} + \vec{k}.$$

The momentum transfers $\vec{\alpha}$ and $\vec{\beta}$ are given by

$$\vec{\alpha} = \vec{\eta} - \left(\frac{v}{2} - \frac{Q}{v} \right) \hat{v}, \quad \vec{\beta} = -\vec{\eta} - \left(\frac{v}{2} + \frac{Q}{v} \right) \hat{v},$$

where $\vec{\eta}$ is the transverse momentum transfer vector with properties $\vec{\alpha} + \vec{\beta} = -\vec{v}$ and $\vec{\eta} \cdot \vec{v} = 0$, and the impact velocity vector \vec{v} is directed along the Z axis. The Q factor of inelasticity is defined as $Q = E_i - (E_{f_1} + E_{f_2})$ for TI and $Q = E_i - (E_{f_1} + E_{f_2})$ for SC, where E_i and E_{f_1}, E_{f_2} are the initial and final binding energies, and $E_{\kappa} = \kappa^2/2$.

The prior transition amplitudes (2.1) and (2.3) contain a term with the factor $(E_i - H_T) \varphi_i(\vec{x}_1, \vec{x}_2)$ with $H_T = -(1/2b) \nabla_{x_1}^2 - (1/2b) \nabla_{x_2}^2 - Z_T/x_1 - Z_T/x_2 + 1/r_{12}$, where $b = m_T/(m_T + 1)$ and m_T is the mass of the target nucleus. If the bound-state wave function for helium were known exactly, the function $\varphi'_i(\vec{x}_1, \vec{x}_2) \equiv (E_i - H_T) \varphi_i(\vec{x}_1, \vec{x}_2)$ would vanish identically. Since such an exact wave function is unavailable, the contribution from $\varphi'_i(\vec{x}_1, \vec{x}_2)$ is not equal to zero. This implies that this term, in principle, should be kept throughout the computation within the prior transition amplitudes $T_{if}^{-(SC)}$ and $T_{if}^{-(TI)}$. This correction was suggested by Belkić [15] within the CB1-4B approximation for double-electron capture. However, numerical computations for double-electron capture [15] and for TI [7] in α -He collisions show that this correction is negligible at high impact energies. For this reason we shall not consider this term in the present paper.

The triple differential cross sections for TI read

$$Q_{if}^{\pm(TI)}(\vec{k}) \equiv \frac{dQ_{if}^{\pm(TI)}}{d\vec{k}} = \int d\vec{\eta} \left| \frac{T_{if}^{\pm(TI)}}{2\pi v} \right|^2, \quad (2.6)$$

whereas the total cross sections are given by

$$Q_{if}^{\pm(TI)} = \int d\vec{k} Q_{if}^{\pm(TI)}(\vec{k}). \quad (2.7)$$

The post and prior total cross sections for SC in the CDW-4B theory are

$$Q_{if}^{\pm(SC)} = \int d\vec{\eta} \left| \frac{T_{if}^{\pm(SC)}}{2\pi v} \right|^2. \quad (2.8)$$

As shown in Ref. [7], after analytical calculations performed by means of the standard Nordsieck technique, the expressions for total cross sections for TI can be reduced to a seven-dimensional numerical integral. In the case of single-charge exchange, the total cross sections are expressed [12,13] via a four-dimensional numerical quadrature.

III. RESULTS AND DISCUSSION

The numerical results for the post (Q_{if}^+) and prior (Q_{if}^-) total cross sections for electron capture from He($1s^2$) to the ground state of Li $^{2+}$ in reaction (1.1) are summarized in Table I and Figs. 1 and 2. In Fig. 1 post and prior cross

sections obtained from the one-parameter orbital for He($1s^2$),

$$\varphi_i(\vec{x}_1, \vec{x}_2) = \frac{\lambda^3}{\pi} e^{-\lambda(x_1 + x_2)}, \quad \lambda = 1.6875, \quad (3.1)$$

are plotted. In this case the post-prior discrepancy does not exceed 26% in the considered energy interval. If the ground state of the helium atom is described by the two-parameter wave function [29]

$$\varphi_i(\vec{x}_1, \vec{x}_2) = \frac{N}{\pi} (e^{-\alpha_1 x_1 - \alpha_2 x_2} + e^{-\alpha_2 x_1 - \alpha_1 x_2}),$$

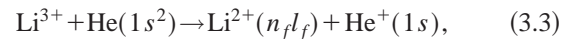
$$N = \left[\frac{1}{\alpha_1^3} + \frac{1}{\alpha_2^3} + \frac{16}{(\alpha_1 + \alpha_2)^3} \right]^{-1/2}, \quad (3.2)$$

the post-prior discrepancy is less significant and does not exceed $\sim 10\%$ (see Table I). The reason for the decreased discrepancy is the fact that the function (3.2) includes some radial static correlations. The discrepancy would disappear if the exact wave function for helium were available.

The CDW-4B total cross sections for the ground-to-ground transition in reaction (1.1) obtained by means of the one-parameter orbital (3.1) and the two-parameter radially correlated orbital (3.2) are very close, as can be seen from Table I. In the case of the post form, the difference between the two corresponding results is less than 7%, while for the prior form the difference is greater, up to 16% (see Table I). The prior cross section is more sensitive to the accuracy of the initial state than the post form, because the expression for the prior amplitude (2.1) does not contain the term $1/r_{12}$, which explicitly accounts for the dynamical correlations.

In Fig. 2, the theoretical post total cross sections for SC to the ground state in Li $^{3+}$ + He collisions are plotted (full line) together with the experimental data of Shah and Gilbody [30] and Voitke *et al.* [31]. As can be seen, the computed cross sections are in satisfactory agreement with the experimental measurements. Our CDW-4B curve lies slightly below the experimental findings, due to the fact that the CDW-4B results displayed include capture only in the ground state, while the contribution from the excited states is accounted for by the factor 1.202 which additionally multiplies the total cross sections. When we neglect the relevant term for dynamic correlations $V(r_{12}, x_1)$ from Eq. (2.4), we obtain cross sections (denoted by Q_{12}^+ in Table I) that grossly underestimate the experimental data (see the dashed curve in Fig. 2). This provides evidence that the dynamic correlations play an important role for electron capture to the ground state, especially at higher impact energies.

In the next stage of investigation we extended the CDW-4B theory for electron capture to the excited states, i.e., for the reaction



where the values of the quantum numbers $n_f l_f$ in this paper are restricted to $1s, 2s, 2p, 3s, 3p,$ and $3d$. The analytical calculations are carried out separately for each subsHELL by means of the partial differentiation technique of the Nords-

TABLE I. Total cross sections (in cm^2) in the CDW-4B model for single-electron capture to the ground state in $\text{Li}^{3+} + \text{He}$ collisions, as a function of incident energy E (keV/amu). The columns labeled Q_{if}^+ and Q_{if}^- correspond to the post and prior results obtained with the complete perturbation potentials according to Eqs. (2.3) and (2.4), while the data Q_P^\pm denote the post (+) and prior (-) cross sections obtained without the term $V_P(R, s_2)$; the symbol Q_{12}^+ refers to the results obtained without the perturbation $V(r_{12}, x_1)$ in Eq. (2.4). The computations carried out by means of the wave functions (3.1) and (3.2) are labeled by (a) and (b), respectively. The results obtained are multiplied additionally by a factor of 1.202 in order to include the contribution from the excited states. The number in square brackets represents the power of 10.

E (keV)/amu		Q_{if}^+	Q_{if}^-	Q_P^+	Q_P^-	Q_{12}^+
50	(a)	1.66[-16]	1.55[-16]	1.15[-16]	1.02[-16]	1.58[-16]
	(b)	1.62[-16]	1.63[-16]	1.14[-16]	1.14[-16]	1.61[-16]
60	(a)	1.40[-16]	1.31[-16]	8.69[-17]	7.65[-17]	1.27[-16]
	(b)	1.38[-16]	1.39[-16]	8.76[-17]	8.82[-17]	1.29[-16]
70	(a)	1.26[-16]	1.19[-16]	7.61[-17]	6.76[-17]	1.08[-16]
	(b)	1.24[-16]	1.26[-16]	7.69[-17]	7.80[-17]	1.09[-16]
90	(a)	1.05[-16]	1.01[-16]	6.67[-17]	6.11[-17]	8.22[-17]
	(b)	1.02[-16]	1.04[-16]	6.65[-17]	6.79[-17]	8.12[-17]
100	(a)	9.14[-17]	9.14[-17]	6.24[-17]	5.78[-17]	7.16[-17]
	(b)	9.14[-17]	9.33[-17]	6.16[-17]	6.31[-17]	7.01[-17]
150	(a)	5.31[-17]	5.18[-17]	4.00[-17]	3.81[-17]	3.59[-17]
	(b)	5.01[-17]	5.13[-17]	3.87[-17]	3.97[-17]	3.43[-17]
200	(a)	2.97[-17]	2.91[-17]	2.42[-17]	2.33[-17]	1.88[-17]
	(b)	2.79[-17]	2.86[-17]	2.34[-17]	2.40[-17]	1.78[-17]
300	(a)	1.06[-17]	1.04[-17]	9.56[-18]	9.23[-18]	6.17[-18]
	(b)	1.00[-17]	1.02[-17]	9.29[-17]	9.49[-18]	5.80[-18]
400	(a)	4.49[-18]	4.38[-18]	4.27[-18]	4.11[-18]	2.42[-18]
	(b)	4.23[-18]	4.32[-18]	4.19[-18]	4.26[-18]	2.27[-18]
500	(a)	2.14[-18]	2.07[-18]	2.12[-18]	2.02[-18]	1.08[-18]
	(b)	2.02[-18]	2.05[-18]	2.09[-18]	2.12[-18]	1.01[-18]
600	(a)	1.11[-18]	1.07[-18]	1.14[-18]	1.08[-18]	5.36[-19]
	(b)	1.05[-18]	1.07[-18]	1.13[-18]	1.15[-18]	4.99[-19]
700	(a)	6.24[-19]	5.91[-19]	6.58[-19]	6.15[-19]	2.85[-19]
	(b)	5.91[-19]	5.98[-19]	6.56[-19]	6.60[-19]	2.65[-19]
800	(a)	3.70[-19]	3.46[-19]	3.98[-19]	3.69[-19]	1.62[-19]
	(b)	3.51[-19]	3.53[-19]	3.99[-19]	4.00[-19]	1.50[-19]
900	(a)	2.30[-19]	2.12[-19]	2.52[-19]	2.31[-19]	9.63[-20]
	(b)	2.18[-19]	2.19[-19]	2.53[-19]	2.53[-19]	8.91[-20]
1000	(a)	1.48[-19]	1.36[-19]	1.65[-19]	1.50[-19]	5.98[-20]
	(b)	1.41[-19]	1.41[-19]	1.66[-19]	1.66[-19]	5.52[-20]
1500	(a)	2.51[-20]	2.18[-20]	2.93[-20]	2.56[-20]	8.68[-21]
	(b)	2.39[-20]	2.34[-20]	3.00[-20]	2.93[-20]	7.95[-21]
2000	(a)	6.56[-21]	5.49[-21]	7.90[-21]	6.67[-21]	2.04[-21]
	(b)	6.30[-21]	6.04[-21]	8.14[-21]	7.82[-21]	1.86[-21]
3000	(a)	9.01[-22]	7.13[-22]	1.12[-21]	9.05[-22]	2.43[-22]
	(b)	8.71[-22]	8.12[-22]	1.16[-21]	1.09[-21]	2.20[-22]
4000	(a)	2.08[-22]	1.59[-22]	2.63[-22]	2.06[-22]	5.14[-23]
	(b)	2.02[-22]	1.85[-22]	2.74[-22]	2.54[-22]	4.65[-23]
5000	(a)	6.52[-23]	4.85[-23]	8.27[-23]	6.37[-23]	1.52[-23]
	(b)	6.37[-23]	5.75[-23]	8.67[-23]	7.94[-23]	1.38[-23]

ieck integrals. As an illustration numerical computations are performed for incident projectile energies 60, 800, and 4000 keV/amu. The results for the state-selective partial cross sections $Q_{n_f l_f m_f}^\pm$ for process (3.3) are given in Table II. Also

reported are the total cross sections Q_{total}^\pm obtained by means of the Oppenheimer $(n_f)^{-3}$ scaling law

$$Q_{\text{total}}^\pm = Q_1^\pm + Q_2^\pm + 2.081 Q_3^\pm, \quad (3.4)$$

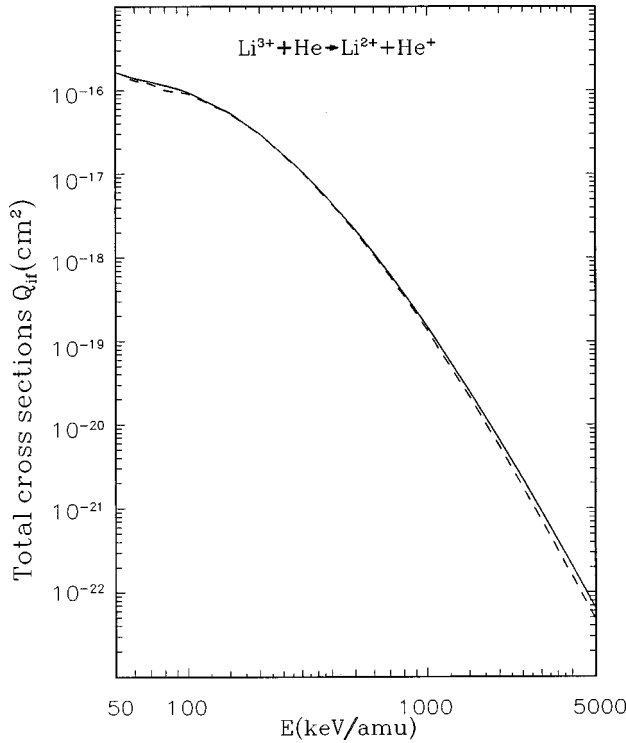


FIG. 1. The total cross sections of the CDW-4B approximation (in cm^2) as a function of the laboratory incident energy E (keV/amu) for the reaction $\text{Li}^{3+} + \text{He} \rightarrow \text{Li}^{2+} + \text{He}^+$. The post cross sections are shown by the full line, while the dashed line represents the prior results. The ground state of the target atom $\text{He}(1s^2)$ is described by means of the one-parameter wave function (3.1).

where the notation $Q_{n_f}^{\pm}$ implies $Q_{n_f}^{\pm} = \sum_{l_f, m_f} Q_{n_f l_f m_f}^{\pm}$. All cross sections given in Table II are obtained assuming the one-parameter orbital (3.1) for $\text{He}(1s^2)$. We have found that electronic correlations remain important for excited states as well. It should be noted that the contribution from the term $V(r_{12}, x_1)$ to the total cross section for the excited states retains a similar trend to that for capture to the ground state. For example, if we compare the post total cross sections computed with and without the term $V(r_{12}, x_1)$, namely, Q_{nl}^+ versus Q_{12}^+ , we obtain, respectively, for $1s$, $2s$, and $3s$ at 4000 keV/amu the values $Q_{nl}^+/Q_{12}^+ = 4.05$, 4.10, and 4.10. These ratios at 800 keV/amu are 2.28, 2.24, and 2.21, whereas at 60 keV/amu they are 1.10, 1.66, and 1.48. The ratio Q_{nl}^+/Q_{12}^+ exhibits similar behavior also for other excited states that are considered in this paper.

The values of the total cross sections (Q_{total}^{\pm}) are displayed in Fig. 2 via the symbol Δ at three selected impact energies. As expected, the contribution from the excited states becomes less important as the impact energy increases. However, at lower energies, total cross sections (Q_{total}^{\pm}) significantly overestimate experimental data in a fashion typical for the CDW approximation. The reason for such behavior can be understood from the following arguments.

(i) The ionization channels dominate over charge exchange at high energies. Therefore, to properly describe electron capture to a final bound state, in the limit of high energies, the electronic-continuum intermediate state must be

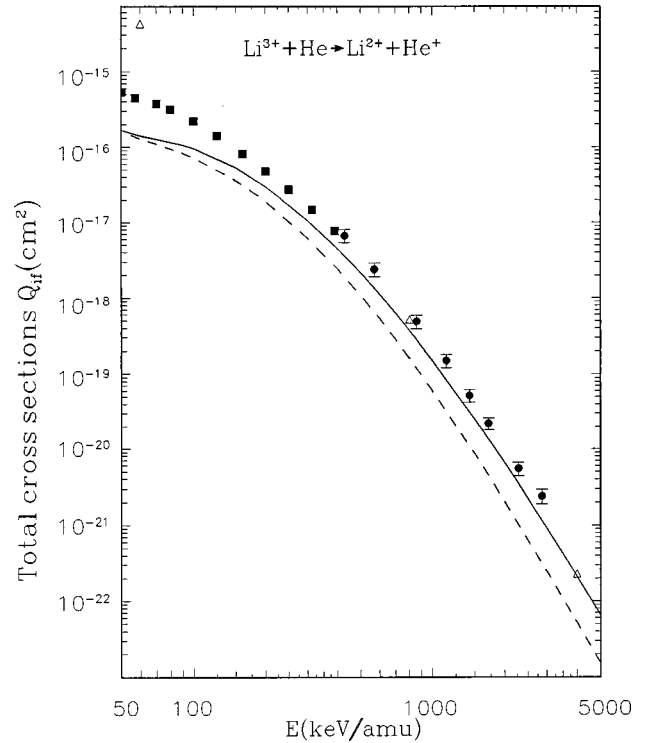


FIG. 2. The total cross sections (in cm^2) as a function of the laboratory incident energy E (keV/amu) for the reaction $\text{Li}^{3+} + \text{He} \rightarrow \text{Li}^{2+} + \text{He}^+$. The full and the dashed lines represent the post cross sections Q_{if}^+ of the CDW-4B method with the complete perturbation potential and without the potential $V(r_{12}, x_1)$, respectively. The symbol Δ refers to theoretical post total cross sections (Q_{total}^+) obtained from Eq. (3.4). The curves correspond to capture into the ground state, while the contribution from the excited states is accounted for by the factor 1.202 which additionally multiplies the total cross sections. The displayed results are obtained by means of the orbital (3.1) for the ground state of the helium target atom. Experimental data: \blacksquare Shah and Gilbody [30]; \bullet Woitke *et al.* [31].

included. This is fully accomplished in the CDW-4B theory, through introduction of the on-shell electronic Coulomb waves centered at Z_P and $(Z_T - 1)$. At lower energies, however, charge exchange dominates over ionization channels. This time, electronic-continuum states represent a drawback, since they overaccount for the intermediate ionization paths of the reaction. Such an observation is supported by the inspection of the Coulomb waves, whose normalization constant increases as the incident energy is decreased. Using these arguments, one can conclude that the CDW method will yield unphysically large cross sections at lower energies. Thus, we should expect, without resorting to any numerical computations, that the neglect of the electronic intermediate ionization states in the channel where distortion is stronger will lead to considerably smaller cross sections, especially at low energies. Such one-channel distorted-wave approaches have been developed for different charge-changing reactions (see, for example, Refs. [32–35], [24], [18], [19]). In our case, the interaction of the projectile (Li^{3+}) with the captured electron is stronger than the interaction between $(Z_T - 1)$ and the captured electron, so that the distortion of the initial bound state is greater than that of the final state.

TABLE II. Total cross sections (in units of cm^2) for reaction (3.3), computed in the CDW-4B approximation. Column labeled $n_f l_f m_f$ refers to the state-selective (partial) cross sections $Q_{n_f l_f m_f}^\pm$. Here we adopt the spectroscopic notation, i.e., $Q_{n_f p}^\pm = Q_{n_f 10}^\pm + 2Q_{n_f 11}^\pm$, $Q_{3d}^\pm = Q_{320}^\pm + 2(Q_{321}^\pm + Q_{322}^\pm)$. Column labeled “total” represents the cross sections Q_{total}^\pm for reaction (3.3), where the summation over the final states is carried out by means of the Oppenheimer $(n_f)^{-3}$ scaling law: $Q_{\text{total}}^\pm = Q_1^\pm + Q_2^\pm + 2.081Q_3^\pm$. The number in square brackets represents the power of 10.

$n_f l_f m_f$	E (keV/amu)					
	60		800		4000	
	post	prior	post	prior	post	prior
100	1.14[−16]	1.07[−16]	3.08[−19]	2.88[−19]	1.73[−22]	1.32[−22]
200	2.11[−16]	2.28[−16]	7.17[−20]	7.00[−20]	2.60[−23]	1.99[−23]
210	7.07[−16]	7.47[−16]	3.19[−20]	3.05[−20]	3.93[−24]	2.82[−24]
211	2.65[−16]	2.50[−16]	1.07[−20]	8.89[−21]	1.58[−24]	1.03[−24]
2p	1.24[−15]	1.25[−15]	5.33[−20]	4.83[−20]	7.09[−24]	4.88[−24]
300	1.32[−16]	1.39[−16]	2.44[−20]	2.41[−20]	8.04[−24]	6.15[−24]
310	2.63[−16]	2.75[−16]	1.23[−20]	1.19[−20]	1.40[−24]	1.03[−24]
311	1.07[−16]	6.69[−17]	4.44[−21]	3.40[−21]	6.20[−25]	3.81[−25]
3p	4.77[−16]	4.09[−16]	2.12[−20]	1.87[−20]	2.64[−24]	1.79[−24]
320	1.16[−16]	1.20[−16]	1.38[−21]	1.31[−21]	4.54[−26]	2.95[−26]
321	1.44[−16]	1.28[−16]	1.81[−21]	1.37[−21]	2.50[−25]	1.35[−25]
322	1.36[−16]	2.67[−17]	6.15[−22]	3.21[−22]	2.57[−26]	7.89[−26]
3d	6.76[−16]	4.29[−16]	6.23[−21]	4.69[−21]	5.97[−25]	4.57[−25]
Total	4.24[−15]	3.62[−15]	5.41[−19]	5.05[−19]	2.30[−22]	1.74[−22]

Therefore, Busnengo *et al.* [24] found good agreement with experimental data including the low-energy region for reaction (3.3) in the framework of the three-body one-channel distorted-wave model (CDW-EIS), when they replaced the continuum distorted factor in the entrance channel by the corresponding logarithmic eikonal phase. The lower limit of application of the CDW-3B theory was established in Ref. [21].

(ii) It should also be noted that at low energies the impact velocity is smaller than the velocity of the electron in the K shell of the target, and thus some molecular effects may become increasingly important. The CDW-4B method does not account for any molecular effects and so it is not expected to be valid at low impact energies.

(iii) The normalization problem of the CDW states causes the total cross sections to be overestimated at intermediate and low energies [36]. This problem is less significant at sufficiently high impact energies. Thus, the CDW-4B model gives reliable cross sections at high velocities where renormalization of the theory is not necessary.

The cross sections for charge exchange to the ground state in reaction (1.1), obtained without the term $V_P(R, s_2)$ in Eqs. (2.3) and (2.4), are denoted in Table I by Q_P^\pm . The computations are carried out with wave functions (3.1) and (3.2) using the post (Q_P^+) and prior (Q_P^-) forms. The influence of the potential $V_P(R, s_2)$ becomes more important with increasing impact energies. For example, the difference between total cross sections obtained with and without this term at 500, 1500, and 5000 keV/amu is 3.4%, 25.2%, and 38.1%, respectively, if the wave function (3.2) is utilized for the ground state of helium. A very similar dependence on

$V_P(R, s_2)$ is observed for the orbital (3.1) (see Table I). We can conclude that for SC to the ground state in $\text{Li}^{3+} + \text{He}$ collisions the contribution of the perturbation $V_P(R, s_2)$ varies by up to 40%. In the case of SC, the x_2 coordinate is small, because the electron e_2 remains bound for the target nucleus, and we can develop $Z_P(1/R - 1/s_2)$ in a power series according to $V_P(R, s_2) = Z_P(1/R - 1/s_2) = Z_P(1/|\vec{s}_2 - \vec{x}_2| - 1/s_2) = Z_P[1/s_2 + \vec{x}_2 \cdot \vec{s}_2/s_2^3 + \dots - 1/s_2] \approx Z_P \vec{x}_2 \cdot \vec{s}_2/s_2^3$. Therefore, the perturbation $V_P(R, s_2)$ should yield a greater contribution to the total cross sections for TI than for SC. Our computations (see Table III and Fig. 3) for process (1.2) confirm that fact; for example, the total cross sections computed with ($Q_{i\bar{p}}^-$) and without ($Q_{\bar{p}}^-$) [the term $V_P(R, s_2)$] in the prior transition amplitude (2.1) differ from each other by at most 67% at 50–5000 keV/amu. The post and prior total cross sections for TI in reaction (1.2), derived with the full perturbations according to Eqs. (2.1) and (2.2), are plotted in Fig. 4, where the experimental findings from Refs. [30], [31] are also displayed. The CDW-4B theory is found to be in good agreement with the experimental data. The post cross sections lie below the prior ones at impact energies between 100 and 3000 keV/amu, with the reverse behavior outside this energy interval. Since the computations for TI are carried out for transfer to the ground state, the agreement with measurements at lower impact energies should be understood in the sense of the previous discussions devoted to the validity of the distorted-wave models for SC in the low-energy region. The theoretical results of Bhattacharyya *et al.* [28] are also depicted in Fig. 4. Their cross sections were computed within a relativistically covariant

TABLE III. The prior Q_{if}^- (cm²) and post Q_{if}^+ (cm²) total cross sections in the CDW-4B theory as a function of the laboratory incident energy E (keV)/amu for transfer ionization in $\text{Li}^{3+} + \text{He}$ collisions. The column labeled Q_P^- corresponds to the results obtained with the assumption $V_P(R, s_2) = 0$ in Eq. (2.1). The ground state of the helium atom is described by the wave function (3.1). The number in square brackets represents the power of 10.

E (keV)/amu	Q_{if}^-	Q_{if}^+	Q_P^-
50	1.2[-16]	1.6[-16]	8.6[-17]
70	9.2[-17]	1.1[-16]	6.7[-17]
100	6.0[-17]	6.2[-17]	4.4[-17]
150	3.1[-17]	2.7[-17]	2.3[-17]
200	1.6[-17]	1.3[-17]	1.2[-17]
400	2.4[-18]	1.6[-18]	2.0[-18]
600	5.8[-19]	3.7[-19]	5.1[-19]
750	2.4[-19]	1.5[-19]	2.3[-19]
1000	6.9[-20]	4.7[-20]	7.3[-20]
1500	1.0[-20]	8.0[-21]	1.3[-20]
2000	2.6[-21]	2.1[-21]	3.4[-21]
3000	3.1[-22]	3.1[-22]	4.8[-22]
4000	6.9[-23]	7.4[-23]	1.1[-22]
5000	2.1[-23]	2.5[-23]	3.5[-23]

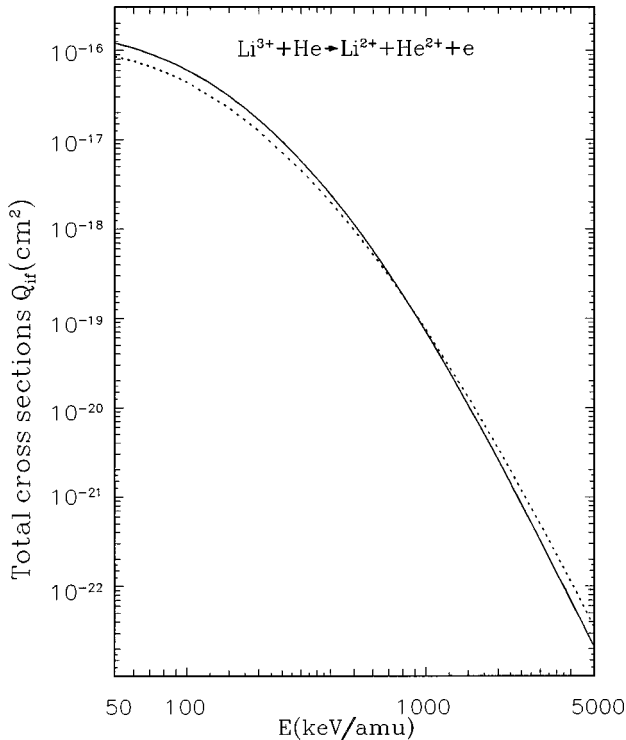


FIG. 3. The total cross sections (in cm²) as a function of the laboratory incident energy E (keV/amu) for the reaction $\text{Li}^{3+} + \text{He} \rightarrow \text{Li}^{2+} + \text{He}^{2+} + e$. The full and dashed curves correspond to the prior total cross sections obtained with the full perturbation potential and neglecting the term $V_P(R, s_2) = Z_P(1/R - 1/s_2)$, respectively. The ground state of the target atom $\text{He}(1s^2)$ is described by means of the wave function (3.1).

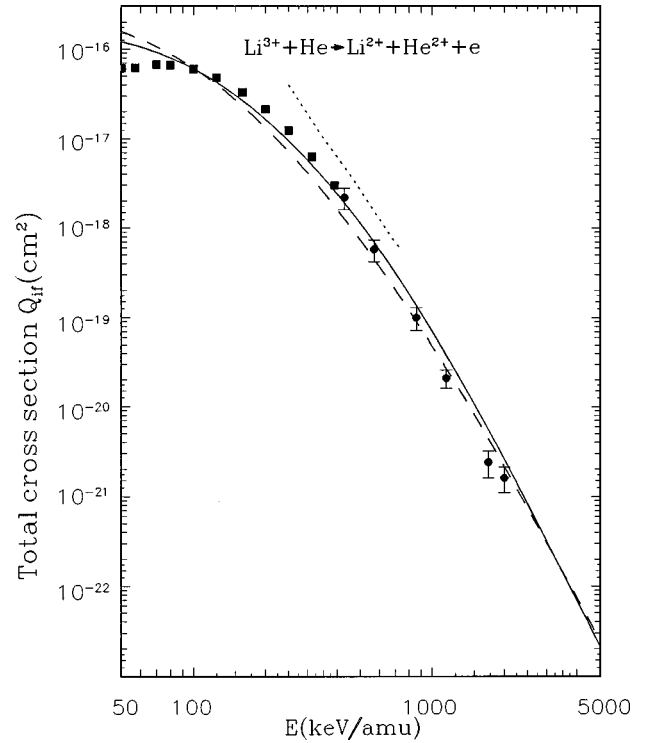


FIG. 4. The total cross sections (in cm²) as a function of the laboratory incident energy E (keV/amu) for the reaction $\text{Li}^{3+} + \text{He} \rightarrow \text{Li}^{2+} + \text{He}^{2+} + e$. The full and dashed lines represent, respectively, the prior Q_{if}^- and post Q_{if}^+ cross sections of the CDW-4B approximation with the complete perturbation potentials. The dotted curve refers to the theoretical results of Bhattacharyya *et al.* [28]. Experimental data: ■ Shah and Gilbody [30]; ● Voitke *et al.* [31].

field approach using the second-order Feynman diagrams. As can be seen from Fig. 4, their results greatly overestimate the experimental measurements.

IV. CONCLUSION

We have investigated the problem of single-electron capture and transfer ionization in the $\text{Li}^{3+} + \text{He}$ collisions by means of the CDW-4B approximation. Numerical computations of the post and prior total cross sections are carried out at impact energies from 50 to 5000 keV/amu. The CDW-4B model explicitly includes the dynamic electronic correlations through the dielectronic interactions $1/r_{12}$ in the transition T operator. The relative importance of the various terms in the perturbation potentials is evaluated. The results obtained indicate that the dynamic electron correlations are very important for capture to the ground state as well as to excited states. The theoretical CDW-4B cross sections for single-electron capture and for transfer ionization are in good agreement with the measurements.

ACKNOWLEDGMENT

Thanks are due to Professor Dževad Belkić for helpful discussions and a critical review of the manuscript.

- [1] J. L. Shinpaugh, J. M. Sanders, J. M. Hall, D. H. Lee, H. Schmidt-Böcking, T. N. Tipping, T. J. M. Zouros, and P. Richard, *Phys. Rev. A* **45**, 2922 (1992).
- [2] V. A. Sidorovich, V. S. Nikolaev, and J. H. McGuire, *Phys. Rev. A* **31**, 2193 (1985).
- [3] R. Shingal and C. D. Lin, *J. Phys. B* **24**, 251 (1991).
- [4] Dž. Belkić and I. Mančev, *Phys. Scr.* **45**, 35 (1992).
- [5] Dž. Belkić and I. Mančev, *Phys. Scr.* **47**, 18 (1993).
- [6] R. Gayet, J. Hanssen, L. Jacqui, A. Martinez, and R. Rivarola, *Phys. Scr.* **53**, 549 (1996).
- [7] Dž. Belkić, I. Mančev, and V. Mergel, *Phys. Rev. A* **55**, 378 (1997).
- [8] I. Mančev, *Nucl. Instrum. Methods Phys. Res. B* **154**, 291 (1999).
- [9] R. Gayet and J. Hanssen, *J. Phys. B* **25**, 825 (1992).
- [10] H. Bachau, R. Gayet, J. Hanssen, and A. Zerarka, *J. Phys. B* **25**, 839 (1992).
- [11] R. Gayet, J. Hanssen, L. Jacqui, and M. Ourdane, *J. Phys. B* **30**, 2209 (1997).
- [12] Dž. Belkić, R. Gayet, J. Hanssen, I. Mančev, and A. Nuñez, *Phys. Rev. A* **56**, 3675 (1997).
- [13] I. Mančev, *Phys. Rev. A* **60**, 351 (1999).
- [14] Dž. Belkić, *J. Phys. B* **26**, 497 (1993).
- [15] Dž. Belkić, *Phys. Rev. A* **47**, 189 (1993).
- [16] I. Mančev, *Phys. Scr.* **51**, 768 (1995).
- [17] I. Mančev, *Phys. Rev. A* **54**, 423 (1996).
- [18] Dž. Belkić, *Phys. Rev. A* **47**, 3824 (1993).
- [19] Dž. Belkić, I. Mančev, and M. Mudrinić, *Phys. Rev. A* **49**, 3646 (1994).
- [20] Dž. Belkić, *Phys. Scr.* **40**, 610 (1989).
- [21] Dž. Belkić, R. Gayet, and A. Salin, *Phys. Rep.* **56**, 279 (1979).
- [22] I. M. Cheshire, *Proc. Phys. Soc. London* **84**, 89 (1964).
- [23] G. S. Saha, S. Data, and S. C. Mukherjee, *Phys. Rev. A* **34**, 2809 (1986).
- [24] H. F. Busnengo, A. E. Martinez, and R. D. Rivarola, *J. Phys. B* **29**, 4193 (1996).
- [25] M. S. Gravielle and J. E. Miraglia, *Phys. Rev. A* **51**, 2131 (1995).
- [26] R. H. Bassel and E. Gerjuoy, *Phys. Rev.* **113**, 749 (1960).
- [27] H. Suzuki, Y. Kajikawa, N. Toshima, H. Ryufuku, and T. Watanabe, *Phys. Rev. A* **29**, 525 (1984).
- [28] S. Bhattacharyya, K. Rinn, E. Salzborn, and L. Chatterjee, *J. Phys. B* **21**, 111 (1988).
- [29] J. N. Silverman, O. Platas, and F. A. Matsen, *J. Chem. Phys.* **32**, 1402 (1960).
- [30] M. B. Shah and H. B. Gilbody, *J. Phys. B* **18**, 899 (1985).
- [31] O. Voitke, P. A. Závodszky, S. M. Ferguson, J. H. Houck, and J. A. Tanis, *Phys. Rev. A* **57**, 2692 (1998).
- [32] Dž. Belkić, *J. Phys. B* **10**, 3491 (1977).
- [33] G. C. Saha, S. Datta, and S. C. Mukherjee, *Phys. Rev. A* **31**, 3633 (1985).
- [34] D. S. F. Crothers and K. M. Dunseath, *J. Phys. B* **15**, 2061 (1982).
- [35] H. F. Busnengo, S. E. Corchs, and R. D. Rivarola, *Phys. Rev. A* **57**, 2701 (1998).
- [36] D. S. F. Crothers, *J. Phys. B* **15**, 2061 (1982); D. S. F. Crothers and J. F. McCann, *ibid.* **18**, 2907 (1985).